Comparative Biochemistry and Physiology, Part B 224 (2018) 88–97

Contents lists available at ScienceDirect

Comparative Biochemistry and Physiology, Part B

journal homepage: www.elsevier.com/locate/cbpb

Metabolic suppression in the pelagic crab, *Pleuroncodes planipes*, in oxygen minimum zones

Brad A. Seibel[a,*], Bryan E. Luu[b,1], Shannon N. Tessier[c,1], Trisha Towanda[d], Kenneth B. Storey[b]

[a] College of Marine Science, University of South Florida, 830 1st St. S., St. Petersburg, FL 33701, USA
[b] Institute of Biochemistry & Department of Biology, Carleton University, 1125 Colonel By Drive, Ottawa, Ontario K1S 5B6, Canada
[c] BioMEMS Resource Center & Center for Engineering in Medicine, Massachusetts General Hospital & Harvard Medical School, 114 16th Street, Charlestown, MA 02129, USA
[d] Evergreen State College, Olympia, WA, USA

ARTICLE INFO

Keywords:
Protein synthesis
Hypoxia
Zooplankton
Hypometabolism
Vertical migration

ABSTRACT

The pelagic red crab, *Pleuroncodes planipes*, is abundant throughout the Eastern Tropical Pacific in both benthic and pelagic environments to depths of several hundred meters. The oxygen minimum zones in this region reaches oxygen levels as low as 0.1 kPa at depths within the crabs vertical range. Crabs maintain aerobic metabolism to a critical PO_2 of ~0.27 ± 0.2 kPa (10 °C), in part by increasing ventilation as oxygen declines. At subcritical oxygen levels, they enhance anaerobic ATP production slightly as indicated by modest increases in lactate levels. However, hypoxia tolerance is primarily mediated via a pronounced suppression of aerobic metabolism (~70%). Metabolic suppression is achieved, primarily, via reduced protein synthesis, which is a major sink for metabolic energy. Posttranslational modifications on histone H3 suggest a condensed chromatin state and, hence, decreased transcription. Under hypoxia, p-H3S10, Ac-H3K9, Ac-H3K14 were 39, 68, and 36% of control values, respectively. We also report a net decrease in protein translation. In particular, eEF2 activity is reduced due to a ~5-fold increase in inhibitory phosphorylation and a significant decrease in protein level. Elevated heat shock proteins suggest that, despite impressive tolerance, the cellular stress response is triggered during hypoxia. We discuss the implications for pelagic ecology and biogeochemical cycles.

1. Introduction

Throughout much of the open ocean, the oxygen content of seawater declines with depth to a minimum value at several hundred meters depth and rises again toward the seafloor. These hypoxic intermediate depths, known as oxygen minimum zones (OMZ), occur where heterotrophic consumption of oxygen outpaces replenishment from atmospheric mixing, photosynthesis or deep-water circulation (Brietburg et al., 2018). OMZs are most pronounced in upwelling regions such as the Eastern Tropical Pacific (ETP) where oxygen values below the surface mixed layer are a small fraction of air saturation. As much as 8% of the world's ocean by volume is characterized by oxygen concentrations < 20 μM (~1.4 kPa PO_2 at 5 °C, Paulmier and Ruiz-Pino, 2009). OMZs are expanding due to reduced solubility in warming waters and to greater stratification of the water column that reduces atmospheric mixing (Brietburg et al., 2018; Keeling et al., 2010; Stramma et al., 2008). Adaptations among midwater animals to these otherwise stable low oxygen conditions include enhanced gill surface areas, high blood-oxygen binding affinity and enhanced capacity for ventilation and circulation (Childress and Seibel, 1998; Seibel, 2011). OMZ inhabitants can thus regulate a constant resting or routine rate of oxygen consumption down to a critical oxygen partial pressure (P_{crit}), below which metabolism can no longer be maintained independent of PO_2. The P_{crits} of OMZ inhabitants are strongly correlated with, and very near, the lowest environmental oxygen values encountered (Childress and Seibel, 1998; Seibel, 2011).

Mesopelagic communities in the most pronounced OMZs are dominated by vertical migrators that move between food-rich, warm, and well-oxygenated surface waters at night and cold, hypoxic and food-poor depths during the daytime. In many species, daylight hours in hypoxia are spent in a metabolically suppressed state (Seibel, 2011). Metabolic suppression, characterized by a total energy demand that is reduced below basal or resting levels, is a common response to temporary resource limitation that permits tolerance to hypoxia, freezing or low food availability (Guppy and Withers, 1999; Hochachka and Somero, 2002). Among oceanic vertical migrators living in pronounced

* Corresponding author.
E-mail address: seibel@usf.edu (B.A. Seibel).
[1] Authors contributed equally.

https://doi.org/10.1016/j.cbpb.2017.12.017
Received 29 July 2017; Received in revised form 19 December 2017; Accepted 20 December 2017
Available online 27 December 2017

OMZs, suppression of total metabolism has now been demonstrated in the jumbo squid, *Dosidicus gigas* (Seibel et al., 2014), the amphipod, *Phronima sedentaria* (Elder and Seibel, 2015a, 2015b), and some krill species (Seibel et al., 2016). Reduced aerobic metabolism during temporary forays into low oxygen has been demonstrated in a few additional zooplankton species (Childress, 1977; Svetlichny et al., 2000; Auel et al., 2005; Maas et al., 2012; Kiko et al., 2015, 2016), but whether they make up the energy deficit anaerobically and, if so, by what pathways, has not been assessed.

Oxygen minimum zones strongly influence the ecology of pelagic ecosystems. The community composition and distribution of species is altered (Prince and Goodyear, 2006; Koslow et al., 2011; Wishner et al., 2013; Maas et al., 2014; Netburn and Koslow, 2015) with consequences for species interactions and the biogeochemical cycles to which they contribute. For example, the consumption of organic carbon in shallow water by vertically-migrating zooplankton, and its subsequent respiration and excretion as carbon dioxide at depth, is thought to contribute significantly to the transport of biological carbon to depth (i.e. the biological pump; Longhurst et al., 1990; Dam et al., 1995; Hays et al., 1997; Steinberg and Landry, 2017 for review). However, estimates of this contribution are based on the assumption that metabolic rates measured at the surface are equivalent, save for the effect of temperature on metabolism, to those exhibited at depth. This assumption may be met by some species in some regions. However, in the Eastern Tropical Pacific, deep-water oxygen levels are below the critical oxygen levels identified for most zooplankton species and respiratory carbon and nitrogen release is suppressed, thus limiting the potential contribution of zooplankton to elemental flux (Seibel, 2011; Seibel et al., 2016; Kiko et al., 2016).

Pleuroncodes planipes, the pelagic red crab, is abundant throughout the eastern Pacific (Gómez-Gutiérrez and Sanchez-Ortiz, 1997) and is a prevalent component in the diets of many oceanic predators including, sharks, tunas, whales and squids (Mathews, 1932; Alverson, 1963; Bazzino et al., 2010; Markaida and Sosa-Nishizaki, 2010; Olson et al., 2014). Under some bloom conditions, these crabs feed primarily by filtering phytoplankton (Longhurst et al., 1967). At other times, they eat protists and zooplankton. They thus form a direct link between primary and secondary producers and their ecologically- and commercially important predators. Its tremendous biomass, estimated at 215,000–611,000 metric tonnes (Gutierrez et al., 2008; De Anda-Montañez et al., 2013, 2016), is evident in the frequent mass strandings that occur on beaches throughout the eastern Pacific (Glynn, 1961; Boyd, 1967; Aurioles-Gaamboa et al., 1994). *P. planipes* is pelagic during at least some phases of their life cycle but its habitat and habits are not fully understood and appear to be plastic (cf: Haye et al., 2010; Roa et al., 1995; Gutierrez et al., 2008; Longhurst, 1966; Boyd, 1967; Aurioles-Gamboa and Pérez-Flores, 1997). They have been observed to depths of at least 385 m (Pineda et al., 2016). Some vertical migration is apparent, but the day-night patterns are variable (Aurioles-Gamboa, 1992; Robinson and Gómez-Gutiérrez, 1998; Robinson et al., 2004; Pineda et al., 2016). Their vertical movements also act as a direct conduit for transfer of carbon and nitrogen from the photic zone to greater depths.

P. planipes encounters extremely low oxygen levels within their vertical range (~0.13 kPa; Pineda et al., 2016) during some, perhaps all, stages of their life. Both juveniles and adults, like its sister species, *P. monodon* (Yannicelli and Castro, 2013; Yannicelli et al., 2013; Kiko et al., 2015), are known to be quite tolerant of hypoxia. Quetin and Childress (1976) reported a P_{crit} near 0.3 kPa (~1.4% of air-saturation). Here we assess the rates of oxygen consumption and ventilation as a function of declining oxygen partial pressure. We further assess the mechanisms and capacity for metabolic suppression in *P. planipes*.

2. Methods

2.1. Collection

Cruises were conducted aboard the *R/V New Horizon* in the Gulf of California, Mexico, in June 2011 and in May 2015 (28°N, 113°W). Additional specimens were collected in the Eastern Tropical Pacific (22° N, 120° W). Specimens were collected either by dipnet at the surface or using a modified, opening-closing Tucker Trawl (Childress et al., 1978) with a $10m^2$ mouth fitted with a 30-l insulated closing cod end. The cod end minimizes temperature changes during recovery to the surface and protects specimens from physical damage due to water turbulence. Opening and closing of the net was triggered electronically using a MOCNESS mechanism (Biological Environmental Sampling Systems). Oxygen profiles in the region were recorded via CTD (conductivity, temperature and depth) casts across the depth range occupied by *Pleuroncodes planipes* (0–400 m). Upon recovery, animals were transferred to air-saturated, filtered seawater and held for a 12-h acclimation period at the measurement temperature (10°) to ensure that animals were post-absorptive.

2.2. Respirometry

After acclimation, specimens were transferred to experimental chambers containing seawater that had been equilibrated with certified gas mixtures of 21 or 1.0 kPa oxygen (balance nitrogen). The actual oxygen concentrations achieved in each chamber (following the transfer of equilibrated water into the experimental chambers) varied slightly and, due to variations in the rate of oxygen consumption between individuals and in the size of the experimental chambers, the ending oxygen concentrations were also variable. Experimental chambers were 50 ml glass syringes or, for larger specimens, 300 ml BOD bottles. Each chamber contained 0.2 μm filtered seawater with 0.5 mg l^{-1} antibiotic (25 mg l^{-1} each, streptomycin and actinomycin) to reduce microbial growth and respiration. Control chambers, containing only seawater (no animal), were incubated simultaneously as a control on microbial respiration and provided the starting oxygen concentration for rate calculations. Following incubation, the chambers were inverted several times to mix the water and water samples (500 μl) were withdrawn from both animal and control syringes and injected past a Strathkelvin oxygen electrode in a water-jacketed housing (Marsh and Manahan, 1999). The difference in oxygen content between the animal and control syringes represents the oxygen consumed. Animals were weighed either at sea on a motion-compensated ship-board balance (Childress and Mickel, 1980) or were frozen and measured subsequently in the home laboratory. Oxygen consumption rates (MO_2) were expressed per gram of wet weight. End-point experiments lasted between 5 and 24 h depending on chamber size and initial experimental PO_2. Experimental temperature (10 °C) was selected to match the daytime temperature to which they are exposed at the deeper end of their diel vertical migration. Oxygen consumption was measured continuously in three specimens to confirm the extremely low P_{crit}, which was measured previously by Quetin and Childress (1976). In those experiments, oxygen was recorded optically using a Witrox microoxygen sensor and oxygen sensitive dot cemented to the inside of a 50 ml glass syringe. Continuous respiration experiments lasted ~24 h while oxygen was consumed completely from a starting PO_2 of 21 kPa. Mixing in these experiments was accomplished via magnetic stir bar. The P_{crit} was determined by determining the intersection in linear regressions between MO_2 (measured every second over the subsequent 5 min) and (PO_2 determined at the initial second of the measurement period) from the regulated (5–10 kPa) and from the conforming (post P_{crit}, estimated visually) parts of the trial.

2.3. Lactate measurement

Additional specimens were incubated in 50 ml syringes as above in hypoxia (PO_2 = 1 kPa) for varying duration (0–24 h) to determine the rate of lactate accumulation. The final oxygen concentration varied but was < 0.1 kPa in all chambers. Lactate was measured as an indicator of anaerobic metabolic energy usage. Following incubations, animals were frozen in liquid nitrogen and stored in the laboratory at − 80 °C until the lactate assays could be performed. Specimens were removed from the freezer and weighed quickly. Tail (abdomen) muscle was excised and homogenized on ice in buffer containing 465 mM NaCl, 19 mM KCl and 20 mM Tris, at pH 7.4. Aliquots (25 µl) of homogenate were placed on test strips and inserted in a Lactate meter (Accutrend (Roche Diagnostics Corp., Indianapolis, USA), which has been used successfully in several studies (Beecham et al., 2006; Elder and Seibel, 2015a; Seibel et al., 2016).

2.4. Calculation of total metabolism

The total metabolic rate includes both aerobic and anaerobic contributions to ATP production. The rate of oxygen consumption provides an estimate of the aerobic component and the ATP produced is calculated assuming 6 ATP per unit O_2 consumed. Anaerobic pathways can be variable with multiple pathways contributing various amounts of ATP per unit end-product accumulated (Hochachka and Somero, 2002). However, in crustaceans, lactate, produced by the conversion of glycolytically-derived pyruvate, is the primary end-product known to accumulate during hypoxic exposure (Spicer et al., 1999; Elder and Seibel, 2015a, 2015b; Seibel et al., 2016) and glycogen is the primary substrate metabolized (Grieshaber et al., 1994). As such, 1.5 mol ATP are produced per mol of lactate accumulated. We used this figure to calculate the anaerobic contribution to total metabolism from the rate of lactate accumulation. Lactate was measured only in abdomen muscle, the largest and most active muscle in the crabs. Thus the calculated contribution of anaerobic metabolism to total metabolism may be an overestimate.

2.5. Ventilation rate

An acrylic flow-through chamber was constructed for video observation of *Pleuroncodes planipes* in varying oxygen concentrations. Chilled water (10 °C) was pumped through a gas-equilibration column to achieve oxygen values ranging from air-saturation (21 kPa) to anoxia (oxygen indistinguishable from zero). Oxygen was recorded using a PreSens optical oxygen probe and meter. A HD video camera was used to film *P. planipes*, which remained stationary on the bottom of the chamber. From a lateral view, scaphognathite ventilation was clearly visible and could be quantified visually from the recordings. Each oxygen level was maintained for 5 min to obtain stable rate measurements.

2.6. Protein extraction

Samples of frozen muscle (~50 mg, sampled from the abdomen) from n = 5 individuals of *Pleuroncodes planipes* from normoxic and hypoxic experimental conditions were separately extracted as per manufacturer's instructions (EMD Millipore; Cat#HOXSTMAG-18 K and Cat#48-615MAG). Briefly, tissue samples were Dounce homogenized 1:3 w:v in ice cold lysis buffer (Millipore; Cat#43-045 or 43-040) containing phosphatase (1 mM Na_3VO_4, 10 mM ß-glycerophosphate) and protease (BioShop Cat# PIC001) inhibitors. After 30 min incubation on ice with occasional vortexing, samples were centrifuged (12,000 × *g*, 20 min, 4 °C) and the supernatants collected as total soluble protein lysates. Protein concentration of the lysates was determined using the Bradford assay (Bio-Rad; Cat# 500-0005) and standardized to 6 µg/µl. Tissue extracts for Luminex® Assays were stored at − 80 °C until further use, while tissue extracts for western blots were combined 1:1 v/v with 2 × SDS loading buffer (100 mM Tris-base pH 6.8, 4% w/v SDS, 20% v/v glycerol, 0.2% w/v bromophenol blue, 10% v/v 2-mercaptoethanol) and boiled. The final protein samples for western blots (3 µg/µl) were stored at − 40 °C until use.

2.7. Luminex® assays

Luminex® assay panels were purchased from EMD Millipore and were used according to the manufacturer's instructions. The assays employed in this study were used to measure oxidative stress enzymes (Oxidative Stress Magnetic Bead Panel, Cat #HOXSTMAG-18 K) and heat shock proteins (Heat Shock Protein Magnetic Bead Panel, Cat#48-615MAG) in *P. planipes* comparing normoxic and hypoxic experimental conditions. Aliquots for Luminex® Assays were either combined with Milliplex MAP Assay Buffer 1 (Cat# 43-010) or Milliplex MAP Assay Buffer 2 (Cat# 43-041) for the Oxidative Stress and Heat Shock Protein panels, respectively. A final working concentration of 3 µg/µl for the Oxidative Stress Panel (75 µg total protein/well) and 60 ng/µl for the Heat Shock Protein Panel (1.5 µg total protein/well) was prepared by diluting lysates at least 1:1 in their corresponding Assay Buffer. Positive and negative controls were also prepared from human cell lines for each multiplex panel. For the Heat Shock Protein panel, these consisted of cell lysates prepared from unstimulated HeLa cells (Millipore Cat# 47-205) versus heat shocked HeLa cells (42 °C for 30 min), grown for 16 h at 37 °C, and treated with arsenite (400 µM for 30 min). For the Oxidative Stress Panel, the controls consisted of unstimulated HepG2 cell lysates (Cat#47-231). Lyophilized cell lysates were reconstituted in 100 µl ultrapure water, gently vortexed, and incubated at room temperature for 5 min. The reconstituted lysates were prepared for use by the addition of an appropriate amount of assay buffer, as specified by manufacturer instructions for each kit.

The protocol for multiplex analysis followed manufacturer's directions. Briefly, premixed antibody capture beads were sonicated, vortexed, and diluted as required. After incubation with assay buffer, sample or control lysates were individually combined with the premixed beads in a 96-well microplate. The assay wells were then incubated on a plate shaker (600–800 rpm) while protected from light for 2 h at room temperature (Oxidative Stress Panel) or overnight at 4 °C (Heat Shock Protein panel). Using a Handheld Magnetic Separator Block (Cat#40-285) to retain the magnetic beads, the assay mixture was subsequently removed, and the wells were then washed three times each with assay buffer. Biotin-labeled detection antibodies were vortexed and diluted as required, and then added to wells containing the magnetic capture beads. After incubation for 1 h at room temperature on a plate shaker protected from light, the wells were decanted, washed, and incubated with appropriately prepared Streptavidin-Phycoerythrin for 15–30 min at room temperature on a plate shaker protected from light. Additionally, amplification buffer was added to each well (15 min incubation at room temperature on a plate shaker) of the Heat Shock Protein Panel before decanting. All wells for both kits were resuspended in Sheath Fluid. Measurements were taken immediately after the assay was finished using a Luminex 200® instrument with xPonent software (Luminex® Corporation).

2.8. Western blotting

The relative expression of proteins and associated posttranslational modifications which are indicative of transcriptional (histone H3) and translational rates (eIF2α, 4E-BP, eEF2) were assessed by western blotting in muscle comparing control and hypoxic sampling points of *Pleuroncodes planipes* (Figs. 1–5). Posttranslational modifications were chosen since they represent molecular indices of chromatin structure and the availability of essential translation initiation and elongation factors. Phosphorylation at serine 10 and acetylation of lysine 9/14 are associated with relaxed chromatin and the activation of transcription

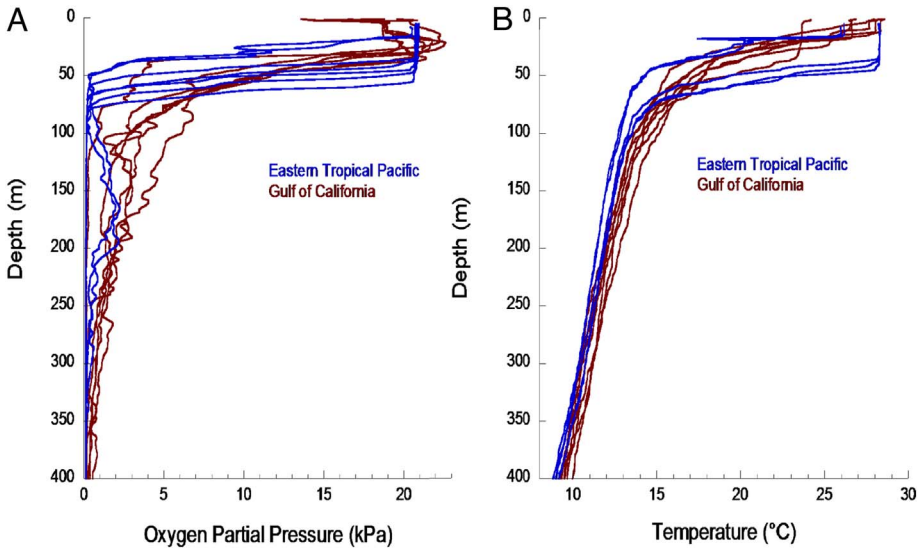

Fig. 1. Temperature (right) and oxygen (left) vs depth profiles in The Eastern Tropical Pacific (blue) and the Gulf of California, Mexico (red). The ETP was slightly cooler at a given depth by ~0.5 °C and was characterized by a much deeper mixed layer and steeper thermocline compared the Gulf of California. A strong oxygen minimum zone was present in both regions. (For interpretation of the references to colour in this figure legend, the reader is referred to the web version of this article.)

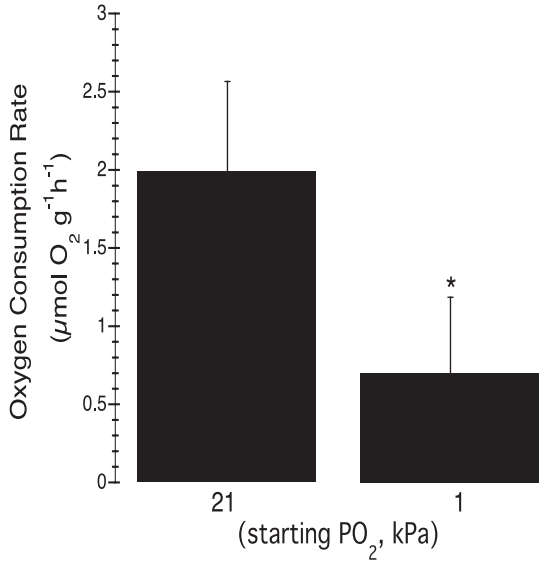

Fig. 2. *Pleuroncodes planipes*: Oxygen consumption rates in closed respiration chambers measured with end-point respirometry at 10 °C. The rates measured with high initial PO_2 (21 kPa, declining to ~11 kPa due to animal consumption) were significantly higher than rates measured with a starting PO_2 of 1 kPa.

(Strahl and Allis, 2000), while the phosphorylation of 4EBP at threonine 45 enhances translation (Gingras et al., 1999) and the phosphorylation of eIF2 at serine 51 (Sudhakar et al., 2000) and eEF2 at threonine 56 (Hizli et al., 2013) are associated with translational suppression.

Equal amounts of protein (20 μg) from each sample were loaded onto 8–15% SDS-polyacrylamide gels and run at 180 V for 45 min in 1 × Tris-glycine SDS running buffer (as described in Seibel et al., 2014). Polyacrylamide gels were made based on a discontinuous gel system; stacking gel pH 6.8 (130 μl 1.0 M Tris-HCl, 170 μl 30% acrylamide, 680 μl water, 10 μl 10% SDS, 10 μl 10% APS, 1 μl TEMED) and conditions for a 10% resolving gel pH 8.8 (1.3 ml 1.5 M Tris-base, 1.7 ml 30% acrylamide, 2.0 ml water, 50 μl 10% SDS, 50 μl 10% APS, 2 μl TEMED). Proteins were then transferred by electroblotting at 160 mA for 1.5 h using transfer buffer (25 mM Tris (pH 8.5), 192 mM glycine and 10% *v*/v methanol) at room temperature. Membranes were blocked with milk (2.5% w:v) made up in TBST (20 mM Tris base, pH 7.6, 140 mM NaCl, 0.05% v/v Tween-20) and were incubated on a rocker for 15 min in order to reduce background and non-specific binding of antibodies.

Membranes were probed with specific primary antibodies, diluted in TBST, at 4 °C overnight. Antibodies were purchased from Cell Signaling (histone H3, 4EBP, eEF2), Assay Designs (HSF1), and GenScript (eIF2α) and were used at 1:1000 v:v dilution in TBST. Additionally, immunoblots were performed using Glyceraldehyde-3-phosphate dehydrogenase (purchased from Santa Cruz Biotechnology, Inc.) antibody as a control in order to observe the stable expression of a housekeeping gene remained constant. Membranes were then probed with HRP-linked anti-rabbit IgG secondary antibody for 1 h (~1:8000 v:v dilution). All membranes were washed 3–6 times between incubation periods in TBST for approximately 5 min per wash. Bands were visualized by enhanced chemiluminescence (H_2O_2 and Luminol) before blots were stained using Coomassie blue (0.25% w/v Commassie brilliant blue, 7.5% v/v acetic acid, 50% methanol) to visualize all protein bands. Antibodies each cross-reacted with strong bands on the immunoblots at the expected molecular masses for histone H3 (17 kDa), 4EBP (19 kDa), eIF2α (36 kDa), eEF2 (95 kDa), and HSF1 (90 kDa).

2.9. Antioxidant capacity assay

The antioxidant capacity was assessed in muscle of *P. planipes* comparing control and hypoxic experimental conditions. The antioxidant assay kit was purchased from Cayman Chemical Company (Cat# 709001, Ann Arbor, MI, USA) and was used according to the manufacturer's instructions. The assay is based on the capacity of antioxidant metabolites present in the sample to prevent ABTS (2,2′-Azino-di-[3-ethylbenzthiazoline sulphonate]) oxidation and this is compared with that of Trolox (values are reported as mM Trolox equivalents).

2.10. Quantification and statistical analysis

Data are expressed as Means ± SEM. Comparisons between oxygen treatments for oxygen consumption rates, lactate concentrations, bead-based assays, normalized band intensities, and antioxidant capacity used a 2-tailed Student *t*-test ($p < 0.05$). Bead-based assays used the net Median Fluorescence Intensity (MFI) of a population of measurements (with a minimum bead count of 50) in order to determine relative protein levels. Band densities on chemiluminescent immunoblots were visualized using a Chemi-Genius BioImaging system (Syngene, Frederick, MD) and quantified using the associated Gene Tools software. Immunoblot band density in each lane was normalized against the summed intensity of a group of Coomassie stained protein bands in

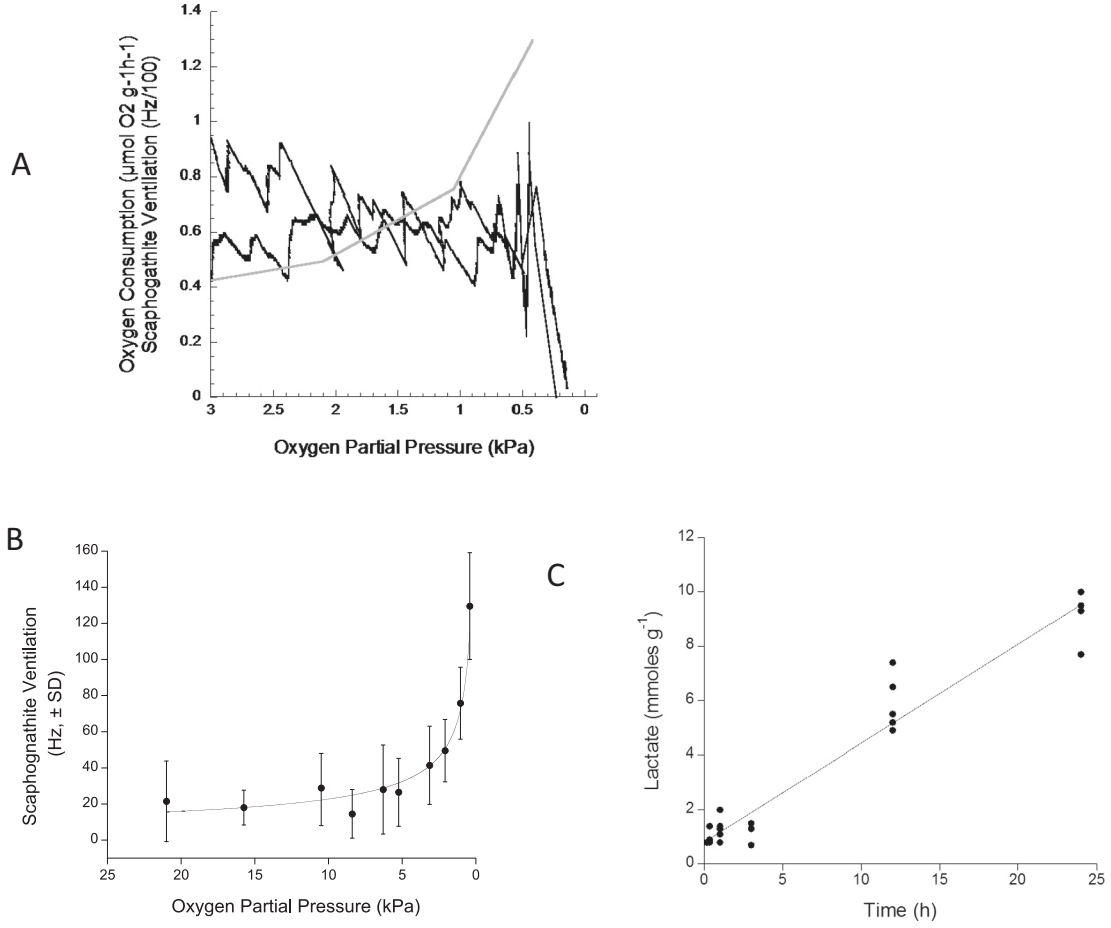

Fig. 3. *Pleuroncodes planipes*: A) Continuous measurement of oxygen consumption rate as a function of PO_2 for two individuals at 10 °C (black lines). The rate of scaphognathite ventilation (grey) is shown on the same figure for comparison. The critical PO_2 (0.4 kPa) measured here at 10 °C is similar to that reported by Quetin and Childress, 1976. B) Scaphognathite ventilation rate as a function of PO_2 (compete curve of that shown in A). D) Lactate accumulation over time at subcritical oxygen levels.

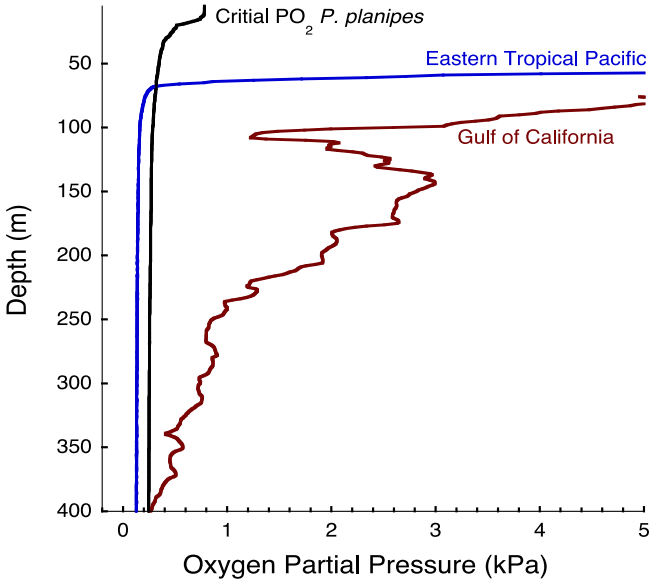

Fig. 4. The critical PO_2 (black) declines with depth due to the effects of temperature (from Quetin and Childress, 1976). A single representative oxygen profile from the ETP and one from the Gulf of California, Mexico are shown for comparison. Where the P_{crit} line intersects with the environmental PO_2 is the critical depth, below which the routine rate of aerobic metabolism can no longer be maintained. Due to the more extreme oxygen minimum zone in the ETP, the critical depth is much shallower (~50–100 m) compared to the Gulf of California (~350 m).

the same lane.

3. Results

3.1. Oxygen and temperature profiles

Temperature profiles were quite similar below the mixed layer in the Gulf of California (GoC) and the Eastern Tropical Pacific (ETP; Fig. 1). The ETP was ~0.5 °C cooler at any given depth and was characterized by a much deeper mixed layer and steeper thermocline. Temperature dropped from ~27 °C at the surface to ~15 °C by 100 m depth. Below the thermocline, temperature declined gradually to about 10 °C at 400 m. A strong oxygen minimum zone was present in both regions. Oxygen partial pressure dropped much more dramatically in the ETP than the GoC, reaching a minimum value of ~0.2 kPa (~1 µM at 10 °C) between 50 and 100 m depth. The PO_2 in the GoC, in contrast, dropped gradually to a similarly low minimum value at about 350 m depth.

3.2. Oxygen consumption rates and critical oxygen partial pressure

Pleuroncodes planipes studied here ranged in mass from 0.106 to 0.511 g wet mass (mean = 0.21 ± 0.11 g). The ending oxygen partial pressure in respirometry chambers that started with air-saturated water was 11.9 ± 2.42 kPa. For hypoxic treatments starting at 1 kPa PO_2, the ending PO_2 was 0.071 ± 0.070 kPa. Routine oxygen consumption rates (MO_2) in air-saturated waters ranged from 0.49 to 2.87 µmol $O_2\ g^{-1}\ h^{-1}$ with a mean of 1.79 ± 0.72 µmol $O_2\ g^{-1}\ h^{-1}$ (n = 16).

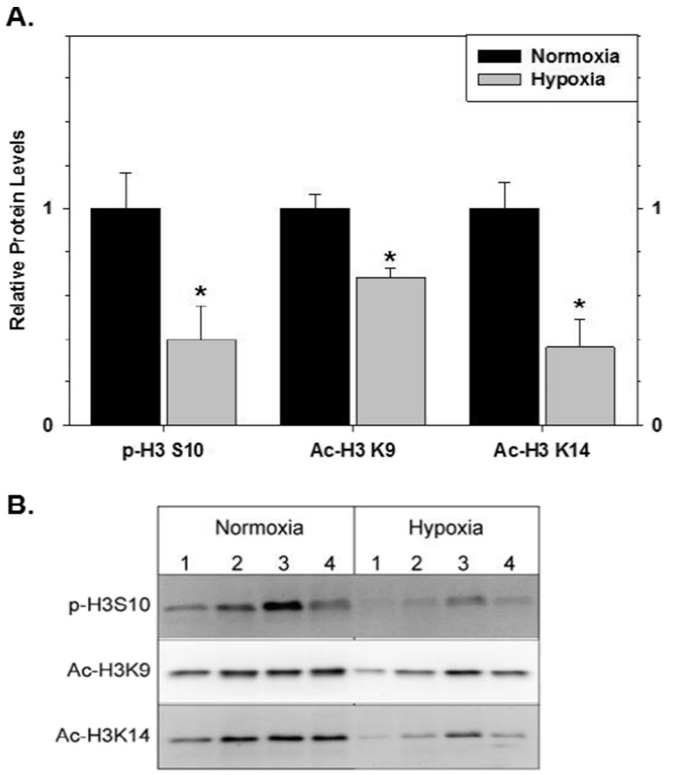

Fig. 5. Relative protein expression of histone H3 and associated posttranslational modifications in muscle of *P. planipes* comparing normoxic and hypoxic experimental conditions. A. Histograms showing relative protein levels were determined using the band densities for immunoblotting. Data are means ± S.E.M. (n = 4–5 independent protein isolations from different animals). B. Representative immunoblots are shown with experimental conditions labeled along the top of the blots. Data were analyzed using a Student *t*-test; * denote values are significantly different from controls ($p < 0.05$).

Hypoxic rates ranged from 0.24 to 1.31 with a mean of 0.58 ± 0.34 μmol O_2 g^{-1} h^{-1} (n = 8) (Fig. 2). This represents a ~70% decline in the rate of aerobic metabolism under hypoxic exposure. The mean critical oxygen partial pressure (P_{crit}) for 3 individuals recorded in the present study (traces for 2 of which are shown in Fig. 3) was 0.40 kPa ± 0.15 kPa, which is within the range reported by Quetin and Childress (1976) (0.13 to 0.46 kPa, mean = 0.27 kPa; 10 °C). The critical depth, defined as the depth at which PO_2 declines below the temperature-adjusted P_{crit}, is illustrated for representative oxygen profiles in the ETP and GoC (Fig. 4). The mean P_{crit}, and the effect of temperature on P_{crit} as reported by Quetin and Childress (1976), were used to calculate the change in P_{crit} across the depth range inhabited by *Pleuroncodes planipes*. A single representative temperature profile from the ETP was used for this calculation. Below the mixed layer, the small differences in temperature (~0.5 °C between the regions studied) had a negligible effect on the P_{crit}. In the ETP, the critical depth, where P_{crit} exceeds environmental PO_2, occurred between 50 and 100 m, while in the GoC the critical depth was below 350 m. As oxygen levels in the respiration chambers approached critical levels, the ventilation rates increased. At 21 kPa PO_2, scaphognathite beat rate was18 ± 9.6 Hz and was stable to PO_2 values approaching 3 kPa. At lower oxygen values the mean ventilation increased dramatically up to 129.5 ± 29.6 Hz near the P_{crit} (Fig. 3). At oxygen levels below P_{crit}, tail muscle lactate accumulated at a steady rate of ~0.3 μmol g^{-1} h^{-1} over 24 h (Fig. 3). Assuming 1.5 ATP mol lactate-1, this equates to ~0.5 μmol ATP g^{-1} h^{-1}.

3.3. Regulation of transcription and translation in response to hypoxia

The relative expression levels of transcription and translation factors were assessed by western blotting. Posttranslational modifications on histone H3, which are associated with a relaxed chromatin state (and hence enhanced transcription), were significantly reduced during hypoxia, as compared to normoxia. These include data for p-H3 S10, Ac-H3 K9, Ac-H3 K14 which were 39, 68, and 36% of control values, respectively. Expression levels of the translation factors eIF2α and its phospho-form did not change, while 4EBP and its phospho-form decreased significantly during hypoxia (values were 50 and 49% of normoxia, respectively) suggesting translational depression. Finally, eEF2 total protein decreased (values were 67% of normoxia) while p-eEF2 T56 increased significantly during hypoxia (values were 4.6-fold higher than controls) also suggesting decreases in translation.

3.4. Response of stress markers during hypoxia

The relative expression levels of antioxidant enzymes were assessed by Luminex® Assays. Fig. 7 shows there was no statistically significant change in the relative expression of catalase, SOD1, SOD2, TRX1 comparing normoxia and hypoxia experimental conditions. Similarly, the antioxidant capacity sustained by multiple targets, including, but not limited to, GSH, Ascorbate, Vitamin E, Bilirubin, and Urate, did not change in muscle during hypoxia as compared to normoxia (Fig. 8). However, it should be noted that total antioxidant capacity may also be influenced by thiol groups of enzymes and structural proteins which also exhibit radical-scavenging activities. In contrast to the response seen for antioxidant enzymes and metabolites, heat shock proteins were much more responsive to hypoxia (Fig. 9). The relative expression levels of HSP proteins were assessed by Luminex® Assays and immunoblotting in *P. planipes* muscle comparing control and hypoxic conditions. While the relative expression of HSF1 did not change, there was a significant increase in the relative protein levels of HSP27, HSP60 and HSP90α during hypoxia; values in hypoxia were 2.7-, 2.0- and 2.6-fold higher than normoxia values, respectively.

4. Discussion

The critical oxygen partial pressure (P_{crit}) reported previously for *Pleuroncodes planipes* (0.27 kPa at 10 °C; Quetin and Childress, 1976) is among the lowest measured for any animal (Fig. 3). In fact, the P_{crit} is below the adaptation threshold suggested by Seibel (2011), an oxygen value (~0.8 kPa, 5 °C) below which few species have evolved mechanisms to regulate their oxygen consumption rate. Our measurements here confirm that previous finding (P_{crit} = 0.4, within the confidence limits of the Quetin and Childress, 1976 measurements). *Pleuroncodes monodon*, a closely related species living in OMZ off the coast of South America, also regulates its oxygen consumption rate to low PO_2 values (< 0.5 kPa; Yannicelli et al., 2013; Kiko et al., 2016). The ability to regulate the respiration rate to such low PO_2 is likely due to exceptional adaptations of the ventilatory and circulatory apparatus. Most species living in pronounced oxygen minimum zones have high ventilatory and circulatory capacities, gills with high surface area and thin membranes that enhance diffusion, a respiratory protein (hemocyanin in this case) with high oxygen affinity and a large Bohr coefficient (pH sensitivity) that facilitates oxygen uptake at the gills and unloading at the tissues (Childress and Seibel, 1998; Seibel, 2011). Most of these parameters have not been measured for *Pleuroncodes planipes*, but Burd (1988) noted enhanced gills in populations of a related species, *Munida quadrispina,* living in a hypoxic fjord. Here we report a dramatic increase in scaphognathite beat (ventilation) rate in *P. planipes* starting at 18 Hz above a PO_2 of ~3 kPa and increasing to ~130 Hz near P_{crit} (Fig. 3C).

Despite a strong oxyregulatory ability, *Pleuroncodes planipes* cannot remain aerobic throughout its entire depth range in the OMZ. It spends considerable time below its critical depth, where environmental PO_2 is below P_{crit}, in some regions (Fig. 4). In air-saturated water, the rate of metabolism at 10 °C was more than three times the hypoxic rates (Fig. 2). At subcritical oxygen levels, anaerobic metabolism increases

but remains a relatively unimportant source of energy (Fig. 3D). *P. monodon* larvae reared in low oxygen increased the activity of lactate dehydrogenase (LDH; Yannicelli et al., 2013), the terminal enzyme in glycolysis that converts pyruvate to lactate to maintain redox balance when oxygen is limiting (Hochachka and Somero, 2002). We show here that anaerobic pathways (lactate) account for ~0.5 μmol ATP g^{-1} h^{-1}. This represents only a small fraction of the ~10 μmol ATP generated via aerobic metabolic pathways in normoxia (10 °C, assuming 6 mol ATP per mol O_2 consumed) and does not make up the deficit in aerobic ATP generation observed under hypoxia. Thus, total metabolism is substantially suppressed (~70%) at oxygen levels below P_{crit}. The disparity between the MO_2 estimated for deep, hypoxic waters and that for shallow waters is even more pronounced when differences in habitat temperature are considered. With temperature coefficients (Q_{10} = factorial change in rate with a 10 °C temperature change) ranging from 1.9–2.5 (Quetin and Childress, 1976), *P.planipes* may exhibit a normoxic routine metabolic rate approaching four times higher at 25 °C, typical of near-surface waters in the ETP, compared to rates in air-saturated water at 10 °C. Normoxic, near-surface rates at high temperature may be 10 × higher than hypoxic rates at depth.

Protein synthesis and gene transcription are energy-expensive processes, consuming a substantial portion of the total ATP turnover of all cells and organs (Hochachka and McClelland, 1997). Reduced ATP consumption serves to protect energy status and fuel stores, and to minimize the accumulation of acidic intermediates of anaerobic ATP-generating pathways during prolonged forays into the OMZ. In the most successful hypometabolic animals, such as turtles that can survive months without oxygen, net metabolic rate suppression is typically 80% and often 95% or more compared with resting metabolism in normoxia. In some cryptobiotic systems, virtually no metabolic activity can be detected. Thus, the 70% suppression of metabolics reported here is relatively modest, but sufficient for short, daytime forays into hypoxic waters. Metabolic suppression is now known to occur in a variety of dominant vertically migrating zooplankton and nekton living in regions with pronounced oxygen minimum zones, including squids (Seibel et al., 2014), krill (Seibel et al., 2016; Kiko et al., 2016), pteropods (Maas et al., 2012), amphipods (Elder and Seibel, 2015b), copepods (Svetlichny et al., 2000; Kiko et al., 2016) and the pelagic crabs reported here (see also, Kiko et al., 2015).

Metabolic suppression is typically achieved via downregulation of energy-intensive cellular processes, such as protein synthesis (transcription and translation) and ion transport (Hand, 1998; Buck and Hochachka, 1993; Storey and Storey, 2004). As is seen in many hypometabolic animal models (Storey and Storey, 2004), *Pleuroncodes planipes* achieves substantial energy savings during exposure to hypoxia by reducing the rate of transcription and translation. Following exposure to subcritical PO_2, posttranslational modifications on histone H3, associated with a relaxed chromatin state and, hence, enhanced transcription (Storey, 2015), were significantly reduced in *P. planipes* abdominal muscle (Fig. 5). These include p-H3 S10, Ac-H3 K9, Ac-H3 K14 which were 39, 68, and 36% of control values, respectively. Thus, reduced transcription appears important in hypoxia-induced metabolic suppression in *P. planipes*. Additionally, the relative expression levels and phosphorylation levels of some translation factors were altered in response to hypoxia (Fig. 6). In particular, we found a net decrease in eEF2 activity, as measured by a very large increase (4.6-fold) in inhibitory phosphorylation and a significant decrease in protein level. Phosphorylation inhibits eEF2 from facilitating the elongation step during protein translation (Hizli et al., 2013). Also, 4EBP is active when phosphorylated, facilitating protein translation (Teleman et al., 2005). Phosphorylation of 4EBP did decrease in hypoxia, but was matched by an equivalent decline in protein level. Similarly, we found no net change in phosphorylation or protein level of eIF2a, which inhibits protein synthesis (Clemens, 2001). While the processes targeted for suppression (e.g. transcription and translation) are common among hypometabolic animals, the molecular route by which metabolic suppression is achieved may differ between species. For example, the primary "chokepoint" in protein translation was through the de-phosphorylation of 4EBP in various squid tissues (Seibel et al., 2014). Other studies in hypoxia-tolerant organisms show that protein synthesis arrest can occur at the stage of transcription or translation (Larade and Storey, 2002; Ivanina et al., 2016). The pelagic crab may rely on hyperphosphorylation of eEF2 to stop overall protein translation by targeting the elongation step. Both routes lead to suppressed protein translation.

We found no change in the relative expression of antioxidant enzymes catalase, SOD1, SOD2, or TRX1 during exposure to hypoxia (Fig. 7). Similarly, levels of antioxidants, including GSH, Ascorbate, Vitamin E, Bilirubin, and Urate, did not change in muscle during hypoxia (Fig. 8). This is in contrast to the response of many hypometabolic and hypoxia-tolerant organisms which often show an increase in Antioxidants and associated enzymes in preparation for oxidative stress (Hermes-Lima and Zenteno-Savin, 2002). Antioxidants and associated enzymes vary seasonally with temperature and, perhaps, food availability in *Pleuroncodes planipes* (Martinez-Canto et al., 2013), conditions that influence metabolic rates. It is surprising that hypometabolism during hypoxia did not result in changes in these parameters. It may be that the levels of antioxidants and antioxidant enzymes are maintained during hypoxia for use during subsequent recovery in warm, well-oxygenated surface waters. However, we have measured only a subset of possible antioxidant responses to hypoxia and other mechanisms for improved ROS scavenging may nonetheless be present. Additionally, while the total protein levels of the antioxidant enzymes may not change, post-translational modifications may alter their activity may modulate the antioxidant response without bulk changes in total protein.

In contrast, we observed a significant increase (2–2.7-fold) in the relative levels of heat-shock protein; HSP27, HSP60 and HSP90α, during hypoxia. Very few studies have addressed the role of heat shock proteins in hypoxia tolerance specifically. However, cross-tolerance, the ability of one stressor to transiently increase tolerance to a second stressor, is thought to involve the induction of HSPs (Todgham and Stillman, 2013). It may be that hypoxia exposure prepares *Pleuroncodes planipes* for subsequent exposure to warm surface waters during recovery and repayment of an oxygen debt as suggested for the squid, *Dosidicus gigas* (Trübenbach et al., 2013a, 2013b). Similarly, in parts of the Eastern Pacific OMZ where sub-critical oxygen levels are found in very shallow waters (Fig. 4), simultaneous exposure to critical temperatures and oxygen levels may be an issue. Elder and Seibel (2015a) reported that extended exposure to temperatures encountered every night during diel migration (~23 °C for *Phronima sedentaria*) is sufficient to induce HSP expression. *P. planipes* regularly experiences high temperatures at the surface (Fig. 1). More likely, however, is that HSPs serve as cytoprotectants during hypometabolism (Storey and Storey, 2011), which would also explain the results of Trübenbach et al. (2013a, 2013b) as squid also strongly suppress metabolism during their diel forays into the OMZ (Seibel et al., 2014). Given the apparent reductions in protein synthesis during hypoxia exposure, stabilizing the existing cellular proteome becomes critical for long-term survival. HSPs act as chaperones that fold new proteins or refold proteins that are damaged and are known to be a universal organismal response to many kinds of stresses that can damage the proteome (Storey and Storey, 2011).

4.1. Expanding oxygen minimum zones, zooplankton migration and biogeochemical cycles

The activity and metabolism of midwater organisms across great depth ranges is believed to play an important role in the transport of carbon and nitrogen from the euphotic zone toward the seafloor and influences the efficiency of carbon sequestration out of the atmosphere (Longhurst and Harrison, 1989; Steinberg and Landry, 2017). Ocean warming and deoxygenation will have important effects on

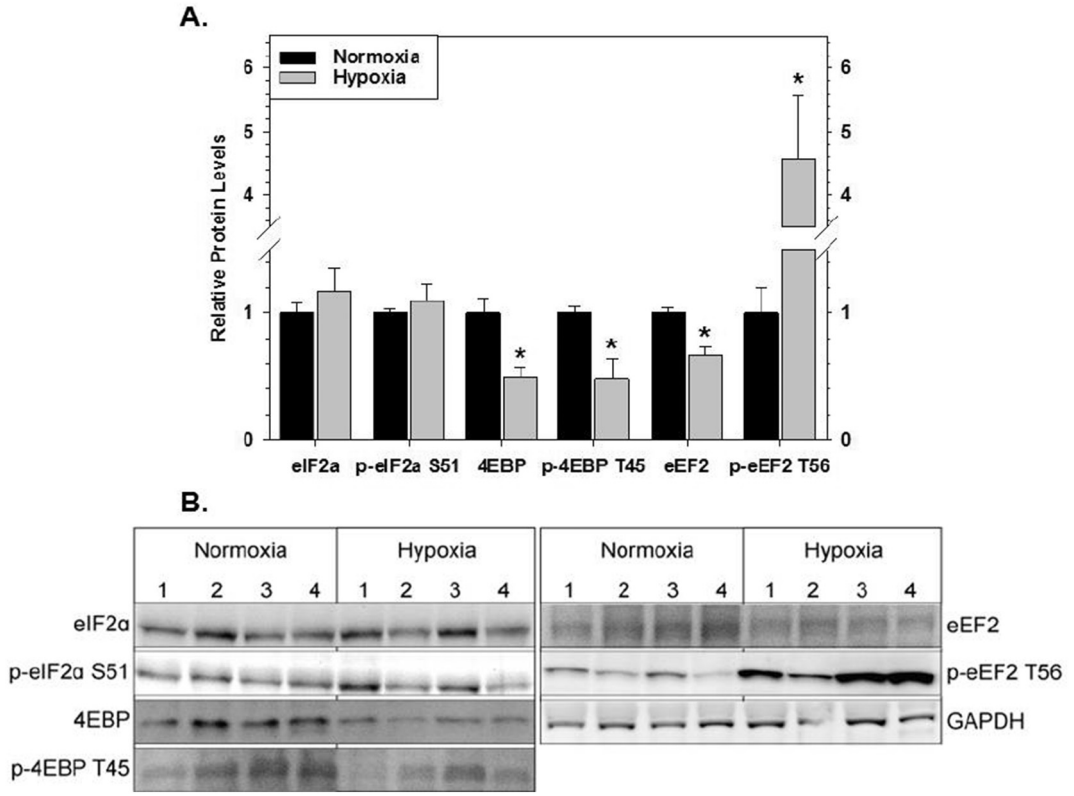

Fig. 6. Relative protein expression of translation initiation and elongation factors in muscle of *P. planipes* comparing normoxic and hypoxic experimental conditions. A. Histograms showing relative protein levels were determined using the band densities for immunoblotting and include eIF2α, 4EBP, and eEF2. Data are means ± S.E.M. (n = 4–5 independent protein isolations from different animals). B. Representative immunoblots are shown with experimental conditions labeled along the top of the blots. All other information as in Fig. 1.

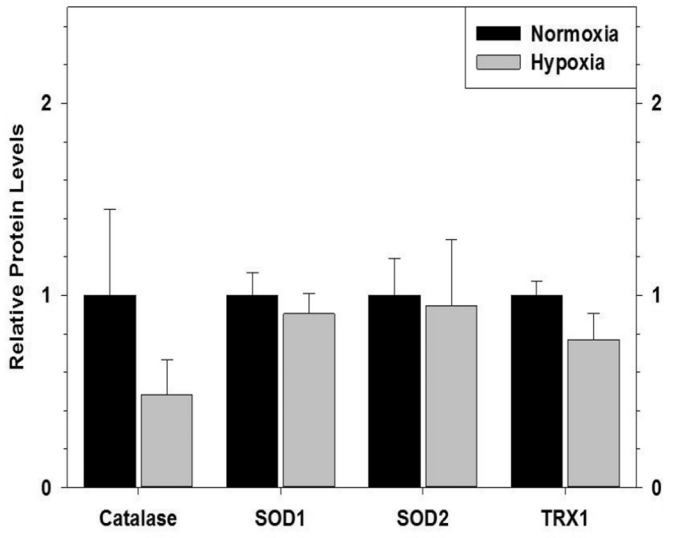

Fig. 7. Relative protein expression of selected antioxidant enzymes in muscle of *P. planipes* comparing normoxic and hypoxic experimental conditions. Histograms showing relative protein levels for bead-based assays were determined using the net MFI as measured by Luminex® and include Catalase, SOD1, SOD2, TRX1. Data are means ± S.E.M. (n = 4–5 independent protein isolations from different animals). All other information as in Fig. 1.

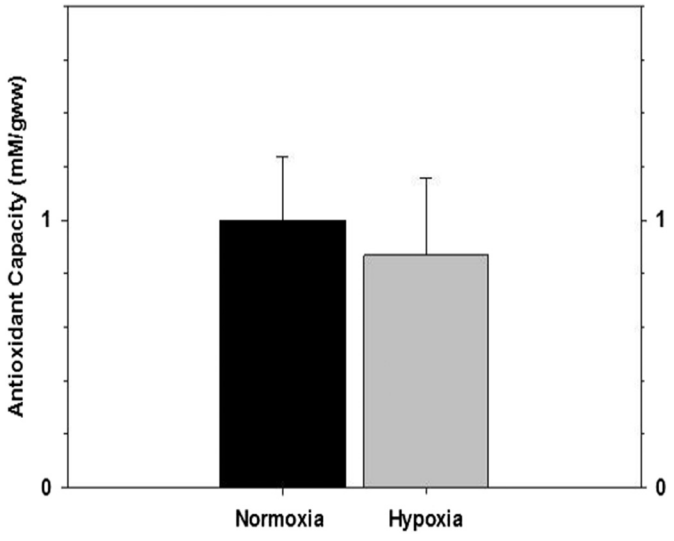

Fig. 8. Antioxidant capacity, measured as equivalents of Trolox (mM/g wet weight), in muscle of *P. planipes* during normoxia and hypoxia experimental conditions. Antioxidants measured in the assay include GSH, Ascorbate, Vitamin E, Bilirubin, and Urate. Histograms show mean ± S.E.M. (n = 4–5 independent protein isolations from different animals). All other information as in Fig. 1.

zooplankton physiology and, thus, biogeochemical cycles (Brietburg et al., 2018; Seibel, 2011). Hypoxia can suppress zooplankton metabolism (Seibel, 2011; Seibel et al., 2014, 2016) as demonstrated here for *Pleuroncodes planipes*, by 50–80%, which reduces the contribution of vertical migrators to carbon and nitrogen flux in regions with strong OMZs by an equivalent amount. The interacting effects of rising temperature and declining oxygen will lead to vertical and latitudinal habitat compression of pelagic species by limiting the depths to which such organisms can migrate during the daytime or requiring that they ascend to shallower depths to acquire sufficient oxygen at night (Fig. 4; Seibel, 2011, 2016; Wishner et al., 2013; Deutsch et al., 2015; Seibel et al., 2016). Higher temperatures in shallower waters will elevate metabolism and increase the critical PO_2, placing a ceiling on the

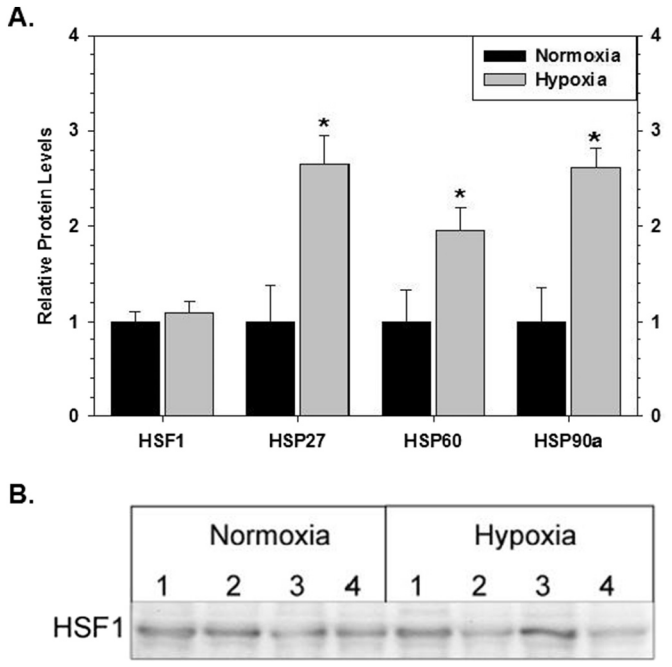

Fig. 9. Relative protein expression of selected heat shock proteins in muscle of *P. planipes* comparing normoxic and hypoxic experimental conditions. A. Histograms showing relative protein levels for bead-based assays were determined using the net MFI as measured by Luminex® (HSP27, HSP60, HSP90α) or band densities for immunoblotting (HSF1). Data are means ± S.E.M. (n = 4–5 independent protein isolations from different animals). B. Representative immunoblots are shown for HSF1 with experimental conditions labeled along the top of the blots. All other information as in Fig. 1.

nighttime habitat depth. Expanding oxygen minimum zones may elevate the floor above which migrators must ascend each night. Climate-induced deoxygenation at deeper depths may limit even their suppressed rate, requiring either more extreme metabolic suppression or greater reliance on anaerobic energy production, thus restricting the duration of their daytime forays into the OMZ.

Acknowledgements

We thank the captain and crew of the R/V *Oceanus* and of the R/V *Sikuliaq* for their assistance at sea. We thank K. Allison Mislan, Agnieszka Dymowska, Yue Jin, Matt Birk, Tracy Shaw and Stephani Gordon for their assistance at sea and in the laboratory and for helpful discussions that improved this manuscript. This work was funded by the National Science Foundation (OCE 1459243 and EF 1316113 grants to B. Seibel). BEL and SNT held NSERC postgraduate and postdoctoral scholarships, respectively.

References

Alverson, F., 1963. The food of yellowfin and skipjack tunas in the eastern tropical Pacific Ocean. Int. Am. Trop. Tuna Comm. Bull. 7, 295–367.
Auel, H., Hagen, W., Ekau, W., Verheye, H.M., 2005. Metabolic adaptations and reduced respiration of the copepod *Calanoides carinatus* during diapause at depth in the Angola-Benguela front and northern Benguela upwelling regions. Afr. J. Mar. Sci. 27, 653–657.
Aurioles-Gaamboa, D., Castro-González, M.I., Pérez-Flores, R., 1994. Annual mass strandings of pelagic red crabs, *Pleuroncodes planipes* (Crustacea, Anomura, Galatheidae), in Bahia Magdalena, Baja California Sur. Mexico. Fish. Bull. 92, 464–470.
Aurioles-Gamboa, D., 1992. Inshore-offshore movements of pelagic red crabs *Pleuroncodes planipes* (Decapoda, Anomura, Galatheidae) off the Pacific coast of Baja California Sur, Mexico. Crustaceana 62, 71–84.
Aurioles-Gamboa, D., Pérez-Flores, R., 1997. Seasonal and bathymetric changes in feeding habits of the benthic red crab *Pleuroncodes planipes* (Decapoda, Anomura, Galatheidae) off the Pacific coast of Baja California Sur, Mexico. Crustaceana 70, 272–287.
Bazzino, G., Gilly, W.F., Markaida, U., Salinas-Zavala, C.A., Ramos-Castillejos, J., 2010. Horizontal movements, vertical-habitat utilization and diet of the jumbo squid (*Dosidicus gigas*) in the Pacific Ocean off Baja California Sur, Mexico. Prog. Oceanogr. 86, 69–71.
Beecham, R.V., Small, B.C., Minchew, C.D., 2006. Using portable lactate and glucose meters for catfish research: acceptable alternatives to established laboratory methods? N. Am. J. Aquac. 68, 291–295.
Boyd, C.M., 1967. The benthic and pelagic habitats of red crab *Pleuroncodes planipes*. Pac. Sci. 21, 394–403.
Brietburg, et al., 2018. Ocean deoxygenation –Causes and consequences in a changing world. Science (In press).
Buck, L.T., Hochachka, P.W., 1993. Anoxic suppression of Na + -K + -ATPase and constant membrane potential in hepatocytes: support for channel arrest. Am. J. Phys. 265, R1020–R1025.
Burd, B.J., 1988. Comparative gill characteristcs of *Munida quadrispina* (Decapoda, Galatheidae) from different habitat oxygen conditions. Can. J. Zool. 66, 2320–2323.
Childress, J.J., 1977. Effects of pressure, temperature and oxygen on the oxygen-consumption rate of the midwater copepod *Gaussia princeps*. Mar. Biol. 39, 19–24.
Childress, J.J., Mickel, T.J., 1980. A motion compensated shipboard precision balance system. Deep-Sea Res. 27, 965–970.
Childress, J.J., Seibel, B.A., 1998. Life at stable low oxygen: adaptations of animals to oceanic oxygen minimum layers. J. Exp. Biol. 201, 1223–1232.
Childress, J.J., Barnes, A.T., Quetin, L.B., Robison, B.H., 1978. Thermally protecting cod ends for the recovery of living deep-sea animals. Deep-Sea Res. 25, 419–422.
Clemens, M.J., 2001. Initiation factor eIF2 alpha phosphorylation in stress responses and apoptosis. Prog. Mol. Subcell. Biol. 27, 57–89.
Dam, H.G., Roman, M.R., Youngbluth, M.J., 1995. Downward export of respiratory carbon and dissolved inorganic nitrogen by diel-migrant mesozooplankton at the JGOFS Bermuda time-series station. Deep Sea Res. Part I: Oceanogr. Res. 42, 1187–1197.
De Anda-Montañez, J.A., Perez-Enriquez, R., Martinez-Aguilar, S., Hernandez-Martinez, F., Garcia-Rodriquez, F.J., Amador-Buenrostro, A., 2013. Abundance and genetic diversity oft he red crab Pleuroncodes planipes along the western coast oft he Baja California Peninsula, Mexico. Fish. Sci. 79, 21–32.
De Anda-Montañez, J.A., Martínez-aguilar, S., Balart, E.F., Zenteno-savín, T., Méndez-rodríguez, L., et al., 2016. Spatio-temporal distribution and abundance patterns of red crab Pleuroncodes planipes related to ocean temperature from the Pacific coast of the Baja California Peninsula. Fish. Sci. 82, 1–15.
Deutsch, C., Ferrel, A., Seibel, B.A., Pörtner, H.O., Huey, R.B., 2015. Climate change tightens a metabolic constraint on marine habitats. Science 348, 1132–1135. http://dx.doi.org/10.1126/science.aaa1605.
Elder, L.E., Seibel, B.A., 2015a. Thermal stress response to diel vertical migration in the hyperiid amphipod, *Phronima sedentaria*. Comp. Biochem. Physiol. A. 187, 20–26. http://dx.doi.org/10.1016/j.cbpa.2015.04.008.
Elder, L.E., Seibel, B.A., 2015b. Ecophysiological implications of vertical migration into oxygen minimum zones for the hyperiid amphipod, *Phronima sedentaria*. J. Plankton Res. 0, 1–15. http://dx.doi.org/10.1093/plankt/fbv066.
Gingras, A.C., Gygi, S.P., Raught, B., Polakiewicz, R.D., Abraham, R.T., Hoekstra, M.F., Aebersold, R., Sonenberg, N., 1999. Regulation of 4E-BP1 phosphorylation: a novel two-step mechanism. Genes Dev. 13, 1422–1437.
Glynn, P.W., 1961. First mass stranding of pelagic crabs (*Pleuroncodes planipes*) at Monterey Bay, California, since 1859 with notes on their biology. Calif. Fish Game 47, 97–107.
Gómez-Gutiérrez, J., Sanchez-Ortiz, C.A., 1997. Larval drift and population structure of the pelagic phase of *Pleuroncodes planipes* (Stimpson) (Crustacea: Galetheidae) off the southwest coast of Baja California, Mexico. Bull. Mar. Sci. 6112 (305-235).
Grieshaber, M.K., Hardewig, I., Kreutzer, U., Pörtner, H.O., 1994. Physiological and Metabolic Responses to Hypoxia in Invertebrates. Rev. Physiol. Biochm. Pharmacol. 125, 43–147 Part of the Reviews of Physiology, Biochemistry and Pharmacology book series (volume 125).
Guppy, M., Withers, P., 1999. Metabolic depression in animals: physiological perspectives and biochemical generalizations. Biol. Rev. Camb. Philos. Soc. 74, 1–40.
Gutierrez, M., Ramirez, A., Bertrand, S., et al., 2008. Ecological niches and areas of overlap of the squat lobster 'munida' (*Pleuroncodes monodon*) and anchoveta (*Engraulis ringens*) off Peru. Prog. Oceanogr. 79, 256–263.
Hand, S.C., 1998. Quiescence in *Artemia franciscana* embryos: reversible arrest of metabolism and gene expression at low oxygen levels. J. Exp. Biol. 201, 1233–1242.
Haye, P.A., Salinas, P., Acuna, E., Poulin, E., 2010. Heterchronic phenotypic plasticity with lack of genetic differentiation in the southeastern Pacific squat lobster *Pleuroncodes monodon*. Evol. Dev. 12, 628–634.
Hays, G.C., Harris, R.P., Head, R.N., 1997. The vertical nitrogen flux caused by zooplankton diel vertical migration. Mar. Ecol. Prog. Ser. 160, 57–62.
Hermes-Lima, M., Zenteno-Savin, T., 2002. Animal response to drastic changes in oxygen availability and physiological oxidative stress. Comp. Biochem. Physiol. C 133, 537–556.
Hizli, A.A., Chi, Y., Swanger, J., Carter, J.H., Liao, Y., Welcker, M., Ryazanolv, A.G., Clurman, B.E., 2013. Phosphorylation of eukaryotic elongation factor 2 (eEF2) by cyclin A- cyclin-dependent kinase 2 regulates its inhibition by eEF2 kinase. Mol. Cell. Biol. 33, 596–604.
Hochachka, P.W., McClelland, G.B., 1997. Cellular metabolic homeostasis during large-scale change in ATP turnover rates in muscles. J. Exp. Biol. 200, 381–386.
Hochachka, P.W., Somero, G.N., 2002. Biochemical Adaptation: Mechanism and Process in Physiological Evolution. Oxford University Press, USA.
Ivanina, A.V., Nesmelova, I., Leamy, L., Sokoov, E.P., Soklova, I.M., 2016. Intermittent hypoxia leads to functional reorganization of mitochondria and affects cellular bioenergetics in marine molluscs. J. Exp. Biol. 219, 1659–1674.
Keeling, R.F., Körtzinger, A., Gruber, N., 2010. Ocean deoxygenation in a warming world.

Annu. Rev. Mar. Sci. 2, 199–229.
Kiko, R., Hauss, H., Dengler, M., Sommer, S., Melzner, F., 2015. The squat lobster, *Pleuroncodes monodon*, tolerates anoxic dead zone conditions off Peru. Mar. Biol. http://dx.doi.org/10.1007/s00227-015-2709-6.
Kiko, R., Hauss, H., Buchholz, F., Melzner, F., 2016. Ammonium excretion and oxygen respiration of tropical copepods and euphausiids exposed to oxygen minimum zone conditions. Biogeosciences 13, 2241–2255. http://dx.doi.org/10.5194/bg-13-2241-2016.
Koslow, J.A., Goericke, R., Lara-Lopez, A., Watson, W., 2011. Impact of declining intermediate-water oxygen on deepwater fishes in the California current. Mar. Ecol. Prog. Ser. 436, 207–218.
Larade, K., Storey, K.B., Storey, K.B., Storey, J.M., 2002. A Profile of the Metabolic Responses to Anoxia in Marine Invertebrates: Chapter 3 in Sensing, Signaling and Cell Adaptation. pp. 27–46.
Longhurst, A.R., 1966. The pelagic phase of *Pleuroncodes planipes* Stimpson (Crustacea, Galatheidae) in the California Current. CalCOFI Reports XI. pp. 142–154.
Longhurst, A.R., Harrison, W.G., 1989. The biological pump: profiles of plankton production and consumption in the upper ocean. Prog. Oceanogr. 22 (1), 47–123.
Longhurst, A.R., Lorenzen, C.J., Thomas, W.H., 1967. The role of pelagic crabs in the grazing of phytoplankton off Baja California. Ecology 48, 190–200.
Longhurst, A.R., Bedo, A.W., Harrison, W.G., Head, E.J.H., Sameoto, D.D., 1990. Vertical flux of respiratory carbon by oceanic diel migrant biota. Deep Sea Res. Part A 37, 685–694.
Maas, A.E., Wishner, K.F., Seibel, B.A., 2012. Metabolic suppression in thecosomatous pteropods as an effect of low temperature and hypoxia in the eastern tropical North Pacific. Mar. Biol. 159, 1955–1967.
Maas, A.E., Frazar, S., Outram, D., Seibel, B.A., Wishner, K.J., 2014. Fine-scale vertical distribution of macroplankton and micronekton in an Eastern Tropical North Pacific in association with an oxygen minimum zone. J. Plankton Res. 0 (0), 1–19. http://dx.doi.org/10.1093/plankt/fbu077.
Markaida, U., Sosa-Nishizaki, O., 2010. Food and feeding habits of the blue shark *Prionace glauca* caught off Ensenada, Baja California, Mexico, with a review on its feeding. J. Mar. Biol. Assoc. UK 90, 977–994.
Marsh, A.G., Manahan, D., 1999. A method for accurate measurements of the respiration rates of marine invertebrate embryos and larvae. Mar. Ecol. Prog. Ser. 184, 1–10.
Martinez-Canto, O., Olguin-Monroy, N.O., Anda-Montanez, J.A., Zenteno-Savin, T., 2013. Spatial and temporal variability of oxidative stress indicators in the red crab, *Pleuroncodes planipes*, from the west coast of the Baja California Peninsula, Mexico. Cienc. Mar. 39, 41–53.
Mathews, L.H., 1932. Lobster-Krill: Anomuran crustacean that are food for whales. Discov. Rep. V, 467–484 (s).
Netburn, A.N., Koslow, J.A., 2015. Dissolved oxygen as a constraint on daytime deep scattering layer depth in the southern California current ecosystem. Deep-Sea Res II: Oceanogr. Res. Papers. 104, 149–158.
Olson, R.J., Duffy, L.M., Kuhnert, P.M., Galván-Magaña, F., Bocanegra-Castillo, N., Alatorre-Ramírez, V., 2014. Decadal diet shift in yellowfin tuna *Thunnus albacares* suggests broad-scale food web changes in the eastern tropical Pacific Ocean. Mar. Ecol. Prog. Ser. 497, 157–178.
Paulmier, A., Ruiz-Pino, D., 2009. Oxygen minimum zones in the modern ocean. Prog. Oceangr. 80, 113–128.
Pineda, J., Cho, W., Starczak, V., Govindarajan, A.F., Guzman, H.M., Girdhar, Y., Holleman, R.C., Churchill, J., Singh, H., Ralston, D.K., 2016. A crab swarm at an ecological hotspot: patchiness and population density from AUV observations at a coastal, tropical seamount. PeerJ 4, e1770. http://dx.doi.org/10.7717/peerj.1770.
Prince, E.D., Goodyear, C.P., 2006. Hypoxia-based habitat compression of tropical pelagic fishes. Fish. Oceanogr. 15, 451–464.
Quetin, L.B., Childress, J., 1976. J. Respiratory Adaptations of *Pleuroncodes planipes* to Its Environment off Baja California.
Roa, R., Gallardo, V.A., Ernst, B., Baltazar, M., Canete, J.I., Enriquez-Brionnes, S., 1995. Nursery ground, age structure and abundance of juvenile squat lobster *Pleuroncodes monodon* on the continental shelf off central Chile. Mar. Ecol. Prog. Ser. 116, 47–54.
Robinson, C.J., Gómez-Gutiérrez, J., 1998. The red-crab bloom off the west coast of Baja California, Mexico. J. Plankton Res. 20, 2009–2016.
Robinson, C.J., Anislado, V., Lopez, A., 2004. The pelagic red crab (*Pleuroncodes planipes*) related to active upwelling sites in the California current off the west coast of Baja California. Deep-Sea Res. II Top. Stud. Oceanogr. 51, 753–766.
Seibel, B.A., 2011. Critical oxygen levels and metabolic suppression in oceanic oxygen minimum zones. J. Exp. Biol. 214, 326–336.
Seibel, B.A., 2016. Cephalopod susceptibility to asphyxiation via ocean incalescence, deoxygenation and acidification. Physiology 31, 418–429.
Seibel, B.A., Häfker, N.S., Trübenbach, K., Zhang, J., Tessier, S.N., Pörtner, H.O., Rosa, R., Storey, K.B., 2014. Metabolic suppression during protracted exposure to hypoxia in the jumbo squid, *Dosidicus gigas*, living in an oxygen minimum zone. J. Exp. Biol. 217, 2555–2568.
Seibel, B.A., Schneider, J., Wishner, K., Kaartvedt, S., Daly, K., 2016. Hypoxia tolerance and metabolic suppression in oxygen minimum zone euphausiids: implications for ocean deoxygenation and biogeochemical cycles. Integr. Comp. Biol. http://dx.doi.org/10.1093/icb/icw091.
Spicer, J.I., Thomasson, M.A., Strömberg, J.O., 1999. Possessing a poor anaerobic capacity does not prevent the diet vertical migration of Nordic krill *Meganyctiphanes norvegica* into hypoxic waters. Mar. Ecol. Prog. Ser. 185, 181–187.
Steinberg, D.K., Landry, M.R., 2017. Zooplankton the ocean carbon cycle. Annu. Rev. Mar. Sci. 9, 413–444.
Storey, K.B., 2015. Regulation of hypometabolism: insights into epigenetic controls. J. Exp. Biol. 218, 150–159.
Storey, K.B., Storey, J.M., 2004. Metabolic rate depression in animals: transcriptional and translational controls. Biol. Rev. Camb. Philos. Soc. 79, 207–233.
Storey, K.B., Storey, J.M., 2011. Heat-shock proteins and hypometabolism: adaptive strategy for proteome preservation. Res. Rep. Biol. 2, 57–68.
Strahl, B.D., Allis, C.D., 2000. The language of covalent histone modifications. Nature 403, 41–45.
Stramma, L., Johnson, G.C., Sprintall, J., Mohrholz, V., 2008. Expanding oxygen-minimum zones in the tropical oceans. Science 320, 655.
Sudhakar, A., Ramachandran, A., Ghosh, S., Hasnain, S.E., Kaufman, R.J., Ramaiah, K.V., 2000. Phosphorylation of serine 51 in initiation factor 2 alpha (eIF2 alpha) promotes complex formation between eIF2 alpha(P) and eIF2B and causes inhibition in the guanine nucleotide exchange activity of eIF2B. Biochemist 39, 12929–12938.
Svetlichny, L.S., Hubareva, E.S., Erkan, F., Gucu, A.C., 2000. Physiological and behavioral aspects of *Calanus euxinus* females (Copepoda: Calanoida) during vertical migration across temperature and oxygen gradients. Mar. Biol. 137, 963–971.
Teleman, A.A., Chen, Y., Cohen, S.M., 2005. 4E-BP functions as a metabolic brake used under stress conditions but not during normal growth. Genes Dev. 19, 1844–1848.
Todgham, A.E., Stillman, J.H., 2013. Physiological responses to shifts in multiple environmental stressors: relevance in a changing world. Integr. Comp. Biol. 53, 539–544.
Trübenbach, K., Pegado, M.R., Seibel, B.A., Rosa, R., 2013a. Ventilation rates and activity levels of jumbo squids under metabolic suppression in the oxygen minimum zone. J. Exp. Biol. 216, 359–368.
Trübenbach, K., Teixeira, T., Diniz, M., Rosa, R., 2013b. Hypoxia tolerance and antioxidant defense system of juvenile jumbo squids in oxygen minimum zones. Deep-Sea Res. Part II: Trop. Stud. Oceanogr. 95, 209–2017.
Wishner, K.F., Outram, D.M., Seibel, B.A., Daly, K.L., Williams, R.L., 2013. Zooplankton in the Eastern Tropical North Pacific: boundary effects of oxygen minimum zone expansion. Deep-Sea Res. I Oceanogr. Res. Pap. 79, 122–140.
Yannicelli, B., Castro, L., 2013. Ecophysiological constraints on the larvae of Pleuroncodes Monodon and the implications for its reproductive strategy in poorly oxygenated waters of the Chile-Peru undercurrent. J. Plankton Res. http://dx.doi.org/10.1093/plankt/fbs090.
Yannicelli, B., Paschke, K., Gonzalez, R.R., Castro, L.R., 2013. Metabolic responses of the squat lobster (Pleuroncodes Monodon) larvae to low oxygen concentration. Mar. Biol. 160, 961–976.